JACS
JOURNAL OF THE AMERICAN CHEMICAL SOCIETY
pubs.acs.org/JACS
Article

π-Extended Rubrenes via Dearomative Annulative π-Extension Reaction

Wataru Matsuoka, Kou P. Kawahara, Hideto Ito,* David Sarlah, and Kenichiro Itami*

Cite This: J. Am. Chem. Soc. 2023, 145, 658−666
Read Online
ACCESS | Metrics & More | Article Recommendations | Supporting Information

ABSTRACT: Among a large variety of organic semiconducting materials, rubrene (5,6,11,12-tetraphenyltetracene) represents one of the most prominent molecular entities mainly because of its unusually high carrier mobility. Toward finding superior rubrene-based organic semiconductors, several synthetic strategies for related molecules have been established. However, despite its outstanding properties and significant attention in the field of materials science, late-stage functionalizations of rubrene remains undeveloped, thereby limiting the accessible chemical space of rubrene-based materials. Herein, we report on a late-stage π-extension of rubrene by dearomative annulative π-extension (DAPEX), leading to the generation of rubrene derivatives having an extended acene core. The Diels−Alder reaction of rubrene with 4-methyl-1,2,4-triazoline-3,5-dione occurred to give 1:1 and 1:2 cycloadducts which further underwent iron-catalyzed annulative diarylation. The thus-formed 1:1 and 1:2 adducts were subjected to radical-mediated oxidation and thermal cycloreversion to furnish one-side and two-side π-extended rubrenes, respectively. These π-extended rubrenes displayed a marked red shift in absorption and emission spectra, clearly showing that the acene π-system of rubrene was extended not only structurally but also electronically. The X-ray crystallographic analysis uncovered interesting packing modes of these π-extended rubrenes. Particularly, two-side π-extended rubrene adopts a brick-wall packing structure with largely overlapping two-dimensional face-to-face π−π interactions. Finally, organic field-effect transistor devices using two-side π-extended rubrene were fabricated, and their carrier mobilities were measured. The observed maximum hole mobility of 1.49×10^{-3} cm^2V^{-1} s^{-1}, which is a comparable value to that of the thin-film transistor using rubrene, clearly shows the potential utility of two-side π-extended rubrene in organic electronics.

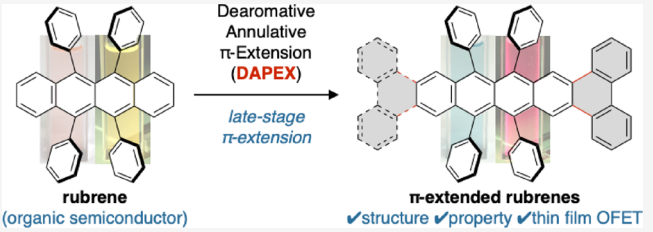

INTRODUCTION

Over the past several decades, π-conjugated compounds such as polycyclic aromatic hydrocarbons have gathered great attention as organic semiconductors (OSCs).[1] OSC-based devices such as organic field-effect transistors (OFETs) and organic light-emitting diodes are generally more flexible, lightweight, and potentially less expensive than their inorganic counterparts.[2] Motivated by such potential applications, the development of efficient synthetic methods for π-conjugated molecules has been intensively investigated.[3] Considering the necessity for evaluating an enormous number of molecules to find an appropriate molecular entity for device applications, late-stage functionalization of existing OSCs can be regarded as one of the most important strategies. Because it would enable chemists to directly install functional groups which perturb the physical properties of a parent molecule, fine-tuning of OSCs can be rapidly carried out without starting their synthesis from scratch.

Among a large variety of OSCs, rubrene (**1**) stands out as a promising molecular entity because of its high carrier mobility in single crystals (Figure 1a).[4] Since a transistor using a single crystal of rubrene was reported to exhibit unusually high carrier mobility (15−40 cm^2/Vs), rubrene has been recognized as the benchmark in this field and has become one of the most frequently studied molecules.[5] During these studies, hundreds of rubrene derivatives have been synthesized and characterized to discover postrubrene materials having enhanced physical properties.[6] As shown in Figure 1b, these derivatives are typically synthesized through an assembly of molecular components by dimerization of propargyl chlorides/alcohols, Diels−Alder reaction of isobenzofuran and aryne, 1,2-addition of organometallic reagents to naphthacenequinone, and cross-coupling reaction of 5,6,11,12-tetrachlorotetracene.[6] However, despite their compelling properties and potential applications to a wide variety of organic electronic materials, late-stage functionalizations of rubrene and its derivatives have been rarely reported,[7] forcing chemists to install functional groups of interest in the early stage of lengthy synthetic protocols. This constraint, which stems from the inertness of C−H bonds and the inherent instability of rubrene toward light and molecular

Received: October 26, 2022
Published: December 23, 2022

https://doi.org/10.1021/jacs.2c11338
J. Am. Chem. Soc. 2023, 145, 658−666

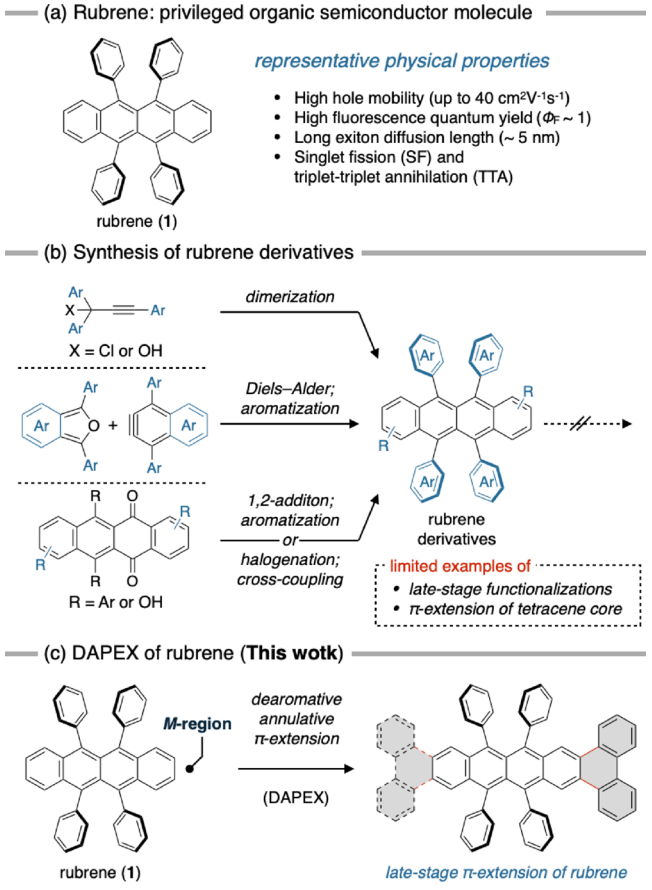

Figure 1. Rubrene (**1**) as a prominent molecular entity for OSCs. (a) Molecular structure of rubrene and representative physical properties. (b) Conventional synthetic strategies for rubrene derivatives. (c) π-Extension of rubrene by DAPEX strategy.

oxygen,[8] often limits the synthetic accessibility of rubrene-based electronic materials. Therefore, strategies for the late-stage functionalizations of rubrene have been highly sought after.

Recently, during our campaign to develop efficient synthetic methods for nanographenes,[9,10] we have reported a unique π-extension method termed as dearomative annulative π-extension (DAPEX).[10] In this method, terminal regions in the longitudinal direction of the acene substructure (*M*-region) of unfunctionalized fused aromatic compounds are selectively π-extended through formal C−H functionalizations. We anticipated that the DAPEX would be a suitable synthetic strategy for the late-stage π-extension of rubrene because (i) rubrene has two *M*-regions at the edge of tetracene core and (ii) the unstable tetracene moiety, which inherently prevents late-stage functionalizations,[8] can be masked by tentative dearomatization[10] (Figure 1c).

In this study, we applied DAPEX to rubrene, and successfully obtained novel rubrene derivatives having pentacene and hexacene cores. Although a major part of rubrene's unique physical properties is provided by its tetracene core, rubrene derivatives having a larger acene core have rarely been synthesized.[11,12] Exceptionally, the family of twistacenes has been synthesized,[12] but these compounds would no longer preserve the unique physical properties of rubrene due to their high distortion of the acene core. Therefore, the present synthetic protocol, which is potentially applicable to the late-stage π-extension of reported rubrene derivatives, would allow chemists to easily explore a new chemical space of π-extended rubrene-based materials. Fundamental properties including photophysical, structural, and semiconducting properties of π-extended rubrenes were investigated, and it was confirmed that one of these compounds (two-side π-extended rubrene) showed semiconducting behavior comparable to rubrene in thin films.

RESULTS AND DISCUSSION

Synthesis of π-Extended Rubrenes. The DAPEX method consists of three fundamental steps: (i) a dearomative [4 + 2] cycloaddition of 4-methyl-1,2,4-triazoline-3,5-dione (MTAD) with aromatic compound;[13] (ii) an iron-catalyzed annulative diarylation, which was originally developed by Nakamura and co-workers;[14] (iii) aromatization by the removal of MTAD.[10] Hence, the DAPEX of rubrene was initiated by the dearomatization of the tetracene core (Figure 2a). As previously reported,[13a] the Diels−Alder reaction of rubrene (**1**) with 1.1 equivalents of MTAD selectively occurred at the terminal benzene ring of the tetracene core to give 1:1 cycloadduct **2** in 90% yield. In addition, the use of an excess amount of MTAD (2.2 equivalents) resulted in the formation of 1:2 cycloadduct **3** as a mixture of *syn*- and *anti*diastereomers. The relative configuration of *syn*-**3** was determined by X-ray crystallographic analysis. Then, the iron-catalyzed annulative diarylation of **2** and the subsequent rearomatization were examined (Figure 2b). Treatment of **2** with biphenyl bis-Grignard reagent **4** in the presence of $Fe(acac)_3$ (acac = acetylacetonato), 1,2-bis(diphenylphosphino)benzene (dppbz), $ZnCl_2$, and 1,2-dichloroisobutane successfully afforded the desired diarylated compound **5** in 70% yield with preferential *exo*selectivity. However, the subsequent rearomatization of **5** under previously reported conditions,[10] where both oxidation and retro-Diels−Alder reactions take place in one-pot by heating with *p*-chloranil, only gave a trace amount of the desired product **6**, probably due to the overoxidation of the product.[15] Therefore, the rearomatization of **5** was redesigned to prevent the overoxidation of **6** as shown in Figure 2b. The oxidation of a diarylated compound **5** without loss of the MTAD moiety would give another precursor **7**. Because this oxidized precursor can be hypothetically rearomatized simply by heating, the π-extended product **6** would be generated in the absence of the oxidant, preventing **6** from the overoxidation. Indeed, similar approaches using a thermally reactive precursor are well investigated in the synthesis of unstable acenes and related compounds,[16] and beneficial for the fabrication of electronic devices. Reaction conditions were investigated, and the oxidation of diarylated compound **5** was successfully achieved by heating with benzoyl peroxide (15 mol %) and *N*-bromosuccinimide (NBS, 1.0 equivalents) at 80 °C to give the oxidized precursor **7** in 52% yield. As expected, the rearomatization of **7** proceeded simply by heating in dibutyl ether (n-Bu_2O) at 170 °C to afford the one-side π-extended rubrene **6** in 86% yield. The two-side π-extended rubrene **9** was also obtained using the same reaction protocol (Figure 2c). Iron-catalyzed annulative diarylation at both activated olefins of 1:2 cycloadduct **3** (1:1 diastereomixture) successfully gave the tetraarylated product in 58% yield. The subsequent oxidation with benzoyl peroxide and NBS afforded the oxidized precursors **8** in 81% total yield. The diastereoisomers of **8** could be easily separated by preparative thin-layer chromatography, giving *syn*-**8** and *anti*-**8** in a 6:4

https://doi.org/10.1021/jacs.2c11338
J. Am. Chem. Soc. 2023, 145, 658−666

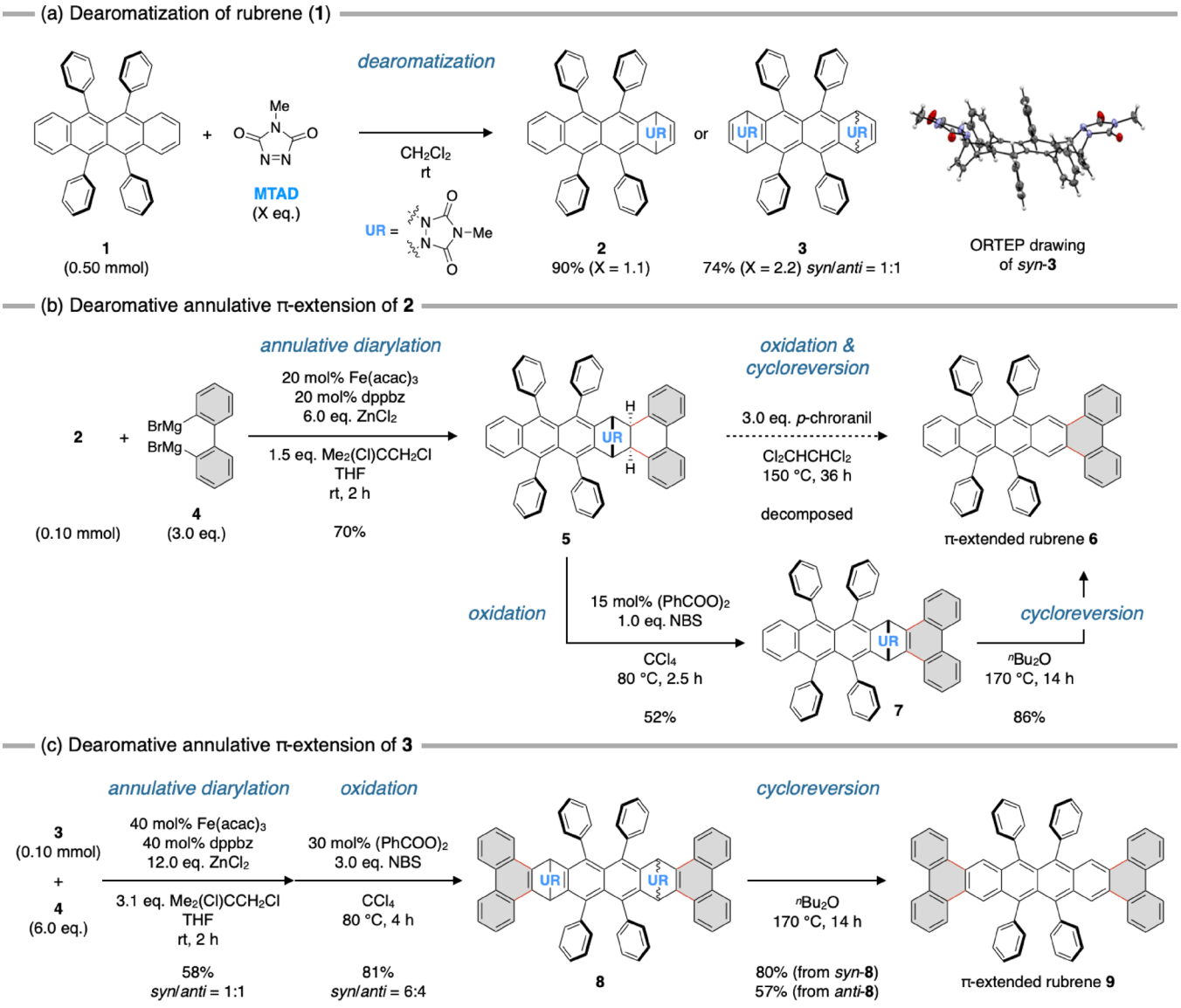

Figure 2. DAPEX of rubrene (**1**). (a) Regioselective dearomative [4 + 2] cycloaddition of MTAD. (b) Annulative diarylation and subsequent rearomatization of cycloadduct **2** to give one-side π-extended rubrene **6**. (c) Annulative diarylation and subsequent rearomatization of cycloadduct **3** to give two-side π-extended rubrene **9**.

diastereomeric ratio, and the relative configuration of *syn*-**8** was determined by X-ray crystallographic analysis (see Supporting Information for details). Finally, the thermal cycloreversion of **8** was performed, and two-side π-extended rubrene **9** was successfully obtained. While the cycloreversion of *syn*-**8** proceeded in good yield (80%), *anti*-**8** only gave the product in 57% yield, probably due to the low reactivity of *anti*-**8** caused by its poor solubility in *n*-Bu_2O.

Photophysical Properties. With the π-extended rubrenes in hand, UV−vis absorption and fluorescence spectra of rubrene (**1**) and π-extended rubrenes **6** and **9** in dichloromethane were measured to elucidate the effect of the π-extension on the electronic properties (Figure 3). While the longest absorption maximum of **1** was observed at 528 nm (ε = 1.07 × 10^4 $cm^{-1}mol^{-1}L$), π-extended rubrenes **6** and **9** have red-shifted absorption maxima at 591 nm (ε = 6.5 × 10^3 $cm^{-1}mol^{-1}L$) and 659 nm (ε = 7.6 × 10^3 $cm^{-1}mol^{-1}L$), respectively (Figure 3a,c). Similar marked red shifts were also observed in the fluorescence spectra of **6** (λ_{em} = 620 nm, Φ_F = 0.45) and **9** (λ_{em} = 682 nm, Φ_F = 0.20) compared to that of **1** (λ_{em} = 557 nm, Φ_F = 0.51) (Figure 3b,c and see SI for further discussions about fluorescence quantum yields (Φ_F) and photostability of the compounds). The fluorescence lifetime (τ_s) of **6** (22.8 ns) was twice as long as that of **1** (11.0 ns), while symmetrically π-extended rubrene **9** showed a slightly shorter lifetime (16.7 ns). To understand the electronic structures, density functional theory (DFT) calculations were performed at the BHandHLYP/TZVP//B3LYP/6-31G(d,p) level of theory.[17] As shown in Figure 3d, both the HOMO and LUMO of **1** are localized on the tetracene core. Similarly, the frontier molecular orbitals of **6** and **9** are localized on the tetracene moieties with small, but nonnegligible contributions from newly constructed benzene rings. The observed longest absorption maxima of these molecules were assigned to the HOMO→LUMO transitions (λ = 508 nm, f (oscillator strength) = 0.2281 for **1**; λ = 571 nm, f = 0.1580 for **6**; λ = 635 nm, f = 0.1187 for **9**) by time-dependent DFT (TD-DFT) calculations. These results, along with the observed marked red

https://doi.org/10.1021/jacs.2c11338
J. Am. Chem. Soc. 2023, 145, 658−666

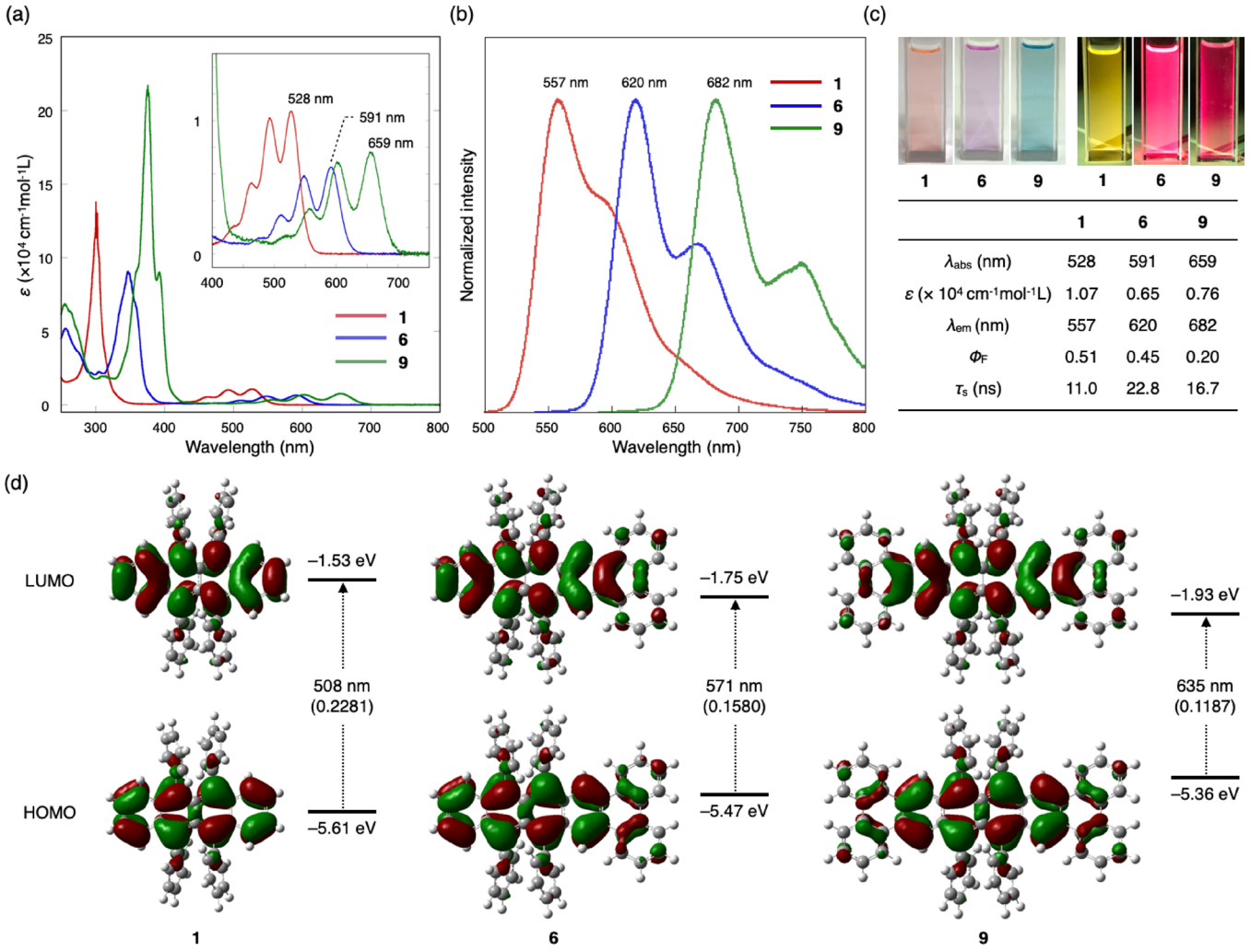

Figure 3. Photophysical properties of rubrene (**1**) and π-extended rubrenes **6** and **9**. (a) UV−vis absorption spectra of **1**, **6**, and **9** in CH_2Cl_2. (b) Normalized emission spectra of **1**, **6**, and **9** in CH_2Cl_2 in the region between λ = 500 and 800 nm. (c) Solution/emission colors of **1**, **6**, and **9** in CH_2Cl_2 and summary of optoelectronic properties. (d) Pictorial frontier molecular orbitals and possible transitions calculated by TD-DFT at the BHandHLYP/TZVP//B3LYP/6-31G(d,p) level of theory.

shift in absorption and emission spectra, indicate that the acene π-system of **1** was successfully extended not only structurally but also electronically.

X-ray Crystallographic Analysis. To disclose the effect of tetracene core π-extension on the molecular and packing structures of rubrene, single crystals of **6** and **9** were grown from diethyl ether and diphenyl ether solution, respectively, and analyzed by X-ray crystallography. The results are shown in Figure 4, along with the reported crystal structure of the parent rubrene (**1**)[5a] and compound **10**, which possesses the common core framework (tetrabenzo[*a*,*c*,*n*,*p*]hexacene moiety) with **9**.[12d] Whereas the tetracene core of **1** is completely planar in the single crystal (ϕ = 0°, where ϕ is an end-to-end dihedral angle defined by four carbon atoms at the edge of an acene moiety), and this nature is believed to contribute largely to its unusually high carrier mobility,[4] the one-side π-extended rubrene **6** has a slightly twisted structure (Figure 4a, ϕ = 17°). The gray-filled triphenylene moiety of **6** is almost planar (ϕ = −5°), and the remaining anthracene moiety is twisted (ϕ = 22°), most likely due to the steric repulsion between the four dangling phenyl groups. On the other hand, the two-side π-extended rubrene **9** was found to have a planar acene core (ϕ = 0°). A structurally similar molecule **10**, reported by Kilway and coworkers, is known as a family of "twistacene" having a largely twisted acene substructure (ϕ = 184°).[12d] With the removal of four phenyl groups at peri positions of **10**, newly synthesized **9** seemed to decrease intramolecular steric repulsions to result in the planar structure, thereby greatly increasing the chance for intermolecular π−π interactions like rubrene.

To analyze the packing structures of these rubrene compounds, we performed the noncovalent interaction plot (NCIPLOT)[18] analysis for **1**, **6**, and **9** which were extracted from the X-ray crystallographic analysis (Figure 4b−d). Regarding the packing structure, **1** is known to adopt the so-called slipped π-stack packing structure,[5a] where largely overlapping intermolecular face-to-face π−π interactions and face-to-edge CH/π interactions exist (Figure 4b).[19] Compound **6** also adopted a similar packing structure as **1**, while both π−π and CH/π interactions of **6** look smaller than those of **1**, resulting in weakened intermolecular interactions in **6** (Figure 4c). On the other hand, two-side π-extended rubrene **9** adopted a brick-wall packing structure with largely overlapping two-dimensional (2D) face-to-face π−π interactions, which is known as one of the most suitable packing structures for the applications in electronic devices (Figure 4d,e).[20] One of the π−π stacking modes is the interaction between blue- and gray-

https://doi.org/10.1021/jacs.2c11338
J. Am. Chem. Soc. 2023, 145, 658−666

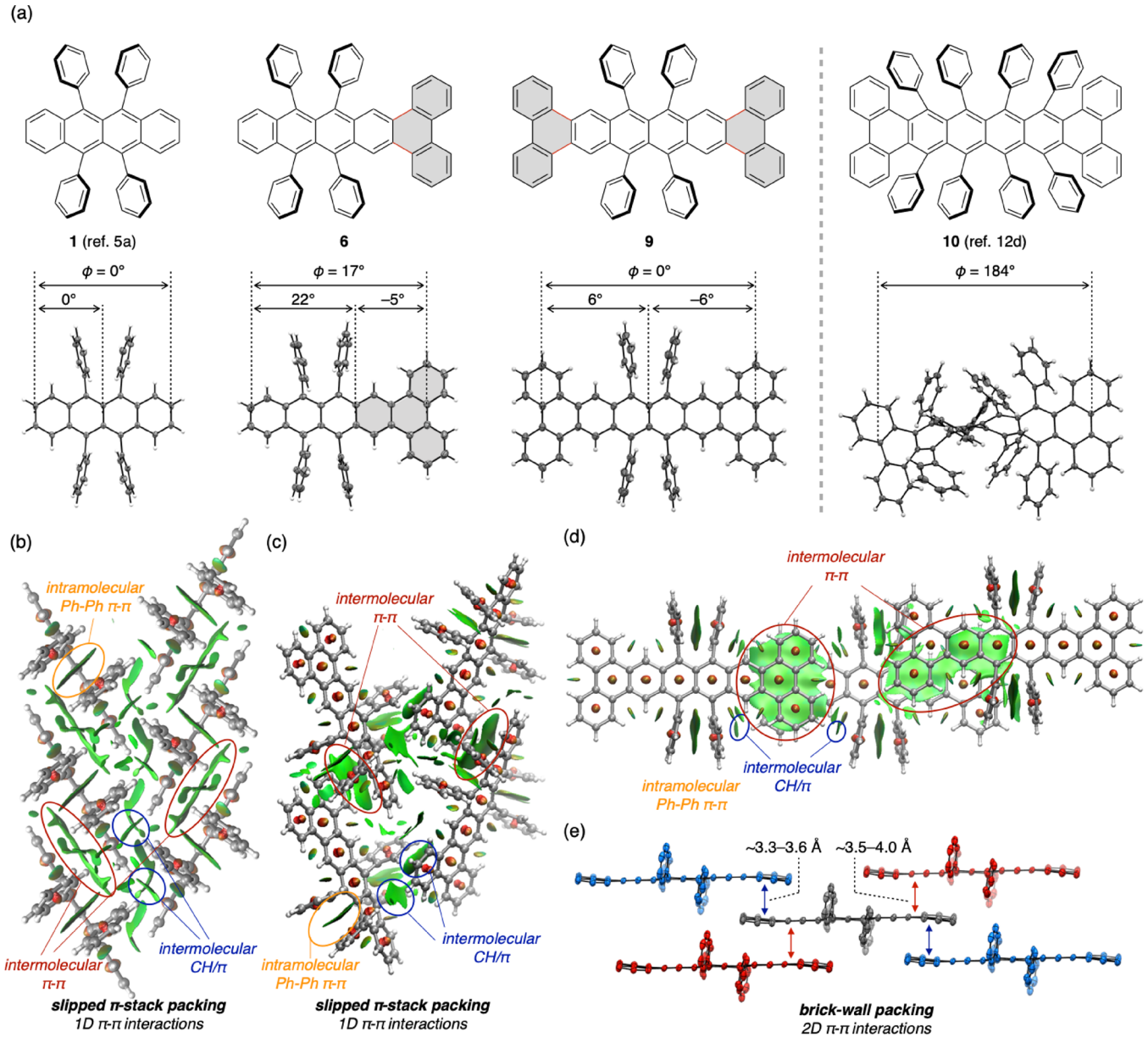

Figure 4. X-ray crystallographic structure of **1**, **6**, **9**, and **10**. (a) Oak Ridge thermal-ellipsoid plot program drawing of the top view. ϕ is an end-to-end dihedral angle of acene cores. NCI analysis and reduced density gradient isosurface (isosurface value = 0.3) by a NCIPLOT4 program for (b) **1**, (c) **6**, and (d) **9**. Color code based on sign $(\lambda_2)\rho$ was −0.7 a.u. (blue) < 0.0 a.u. (green) < 0.7 a.u. (red). Blue and red isosurfaces show regions having attractive and repulsive interactions, respectively, and green isosurfaces show week van der Waals interactions such as $\pi-\pi$ interaction. Each structure was extracted from the data of X-ray crystallographic analyses. (e) Crystal packing structure of **9**. Hydrogen atoms in the packing structure of **9** and solvent molecules in the NCI plot of **6** are omitted for clarity.

colored molecules in which the terminal phenanthrene moieties are overlapped with each other. The other mode is the stacking between red- and gray-colored molecules, where terminal benzene rings interact with naphthalene moieties in the middle of the hexacene core (Figure 4e). The distances between the closest pair of carbon atoms in each stacking mode were estimated to be 3.32 and 3.45 Å, respectively, indicating the existence of moderate to strong $\pi-\pi$ interactions. Through these $\pi-\pi$ interactions, one molecule of **9** can interact with four neighboring molecules (Figure 4e), forming a 2D network of $\pi-\pi$ interactions. It should be noted that, among a large variety of rubrene derivatives reported to date,[6] only a few molecules are found to adopt this packing structure,[21] and that compound **9** is, to the best of our knowledge, the first example of an electronically unbiased rubrene derivative having 2D $\pi-\pi$ interactions in the crystal structure. The observed change in packing structures from **1** to **9** might be understandable by analogy of a well-known crystal engineering strategy for 6,13-bis((trialkylsilyl)ethynyl)-pentacenes (TAS-pentacenes).[22] Anthony and coworkers revealed that the packing structure of TAS-pentacene is determined by the ratio of the diameter of trialkylsilyl groups (r) at peri positions to the length of the acene core (L), and the brick-wall packing structure would be observed when this ratio (r/L) becomes close to 0.5.[22] Considering the similarity in molecular structures of rubrene and TAS-pentacene, DAPEX of **1** caused the increase of the length of the acene core (L), while keeping the size of substituent at peri positions

https://doi.org/10.1021/jacs.2c11338
J. Am. Chem. Soc. 2023, 145, 658−666

(phenyl groups) unchanged, resulting in an appropriate ratio of r to L.

Evaluation of Hole Mobility. Because the observed brick-wall packing structure of two-side π-extended rubrene **9** is believed to contribute to the high carrier mobility in thin-film OFET using prominent OSCs such as TIPS-pentacene, oxo(phthalocyaninato)titanium (TiOPc), and *N*,*N*′-bis-(cyclohexyl) naphthalene-1,4,5,8-bis(dicarboximide),[20,22,23] OFET devices using **9** were fabricated, and their carrier mobilities were measured. The *p*-type OFET devices were fabricated in the top-contact/bottom-gate (TC/BG) configurations, and a thin film of **9** was formed by vapor deposition on the SiO_2 substrate treated with octadecyltrimethoxysilane (see SI for detailed procedure). To our delight, the thin-film layer of compound **9** showed semiconducting behavior, and the average hole mobility for 16 independent devices was estimated to be 7.11×10^{-4} cm^2V^{-1} s^{-1} with a threshold voltage of −4.7 V and on/off current ratio of 1.8×10^4 (Table 1, entry 1). Although the device performance was only moderately good, the hole mobility could be improved by thermal annealing (entries 2−5). The maximum hole mobility of 1.49×10^{-3} cm^2V^{-1} s^{-1}, which is a comparable value to the thin-film transistor using rubrene (2.71×10^{-3} cm^2V^{-1} s^{-1}, entry 6), was observed when the thin film was annealed at 140 °C for 15 min (entry 4). The thermal stability of compound **9** was confirmed by thermogravimetry-differential thermal analysis (TG-DTA, see SI), where no decomposition and no enthalpy change of compound **9** occurred bellow 400 °C, indicating that the observed change in hole mobilities could be accounted by a subtle change in aggregation morphology around the substrate surface. The transfer and output characteristics of this device are shown in Figure 5. Although a comparison of hole mobilities in the single crystal could not be carried out due to the difficulty in preparing devices, the results described above could imply the possibility of two-side π-extended rubrene **9** as a novel class of rubrene-based OSCs with comparable mobility to rubrene.

Table 1. OFET Performance of Compound 9 and Rubrene (1)

entry	T^a (°C)	$\mu_{ave}{}^b$ (cm^2/VS)	$\mu_{max}{}^c$ (cm^2/VS)	$V_{th}{}^d$ (V)	on/off ratio^e
1		7.11×10^{-4}	7.69×10^{-4}	−4.7	1.8×10^4
2	100	6.26×10^{-4}	6.98×10^{-4}	−5.7	1.6×10^4
3	120	7.76×10^{-4}	1.12×10^{-3}	−7.4	1.7×10^4
4	140	7.28×10^{-4}	1.49×10^{-3}	−7.1	4.0×10^3
5	160	6.72×10^{-4}	8.42×10^{-4}	−7.9	6.3×10^3
6^f		2.62×10^{-3}	2.71×10^{-3}	−3.3	2.1×10^5

[a]Annealing temperature. [b]Average hole mobility over five independent devices. [c]Maximum hole mobility over five independent devices. [d]Average threshold voltage over five independent devices. [e]Average on/off current ratio over five independent devices. [f]Rubrene (**1**) was used instead of compound **9**.

CONCLUSIONS

In conclusion, we have applied our DAPEX method to one of the promising OSCs, rubrene, and successfully obtained π-extended rubrene derivatives **6** and **9**. The Diels−Alder reaction of rubrene with MTAD occurred selectively at the terminal benzene ring of the tetracene core to give 1:1 and 1:2 cycloadducts which further underwent iron-catalyzed annulative diarylation with the biphenyl bis-Grignard reagent. The thus-formed 1:1 and 1:2 adducts were subjected to radical-mediated oxidation and thermal cycloreversion to furnish one-side and two-side π-extended rubrenes **6** and **9**, respectively. These π-extended rubrenes **6** and **9** displayed a marked red shift in absorption and emission spectra, clearly showing that the acene π-system of rubrene was extended not only structurally but also electronically. The X-ray crystallographic analysis uncovered interesting packing modes of these π-extended rubrenes. Particularly, two-side π-extended rubrene **9** adopts a brick-wall packing structure with largely overlapping 2D face-to-face $\pi-\pi$ interactions, which is known as one of the most suitable packing structures for applications in electronic devices. Finally, the OFET devices using two-side π-extended rubrene **9** were fabricated, and their carrier mobilities were measured. The observed maximum hole mobility of 1.49×10^{-3} cm^2V^{-1} s^{-1}, which is a comparable value to a thin-film transistor using rubrene, clearly shows the potential utility of two-side π-extended rubrene in organic electronics. The established synthetic method not only represents one of the limited examples of late-stage functionalization of rubrene, but also enables access to a previously untapped chemical space of rubrene derivatives having a larger acene core.

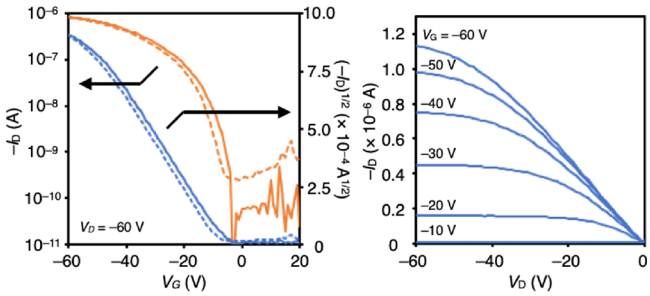

Figure 5. Transfer (left) and output (right) characteristics of the TC/BG device for the thin-film layer of compound **9** prepared by vapor deposition followed by thermal annealing at 140 °C for 15 min.

ASSOCIATED CONTENT

Supporting Information

The Supporting Information is available free of charge at https://pubs.acs.org/doi/10.1021/jacs.2c11338.

Experimental procedures, preparation of Grignard reagents, synthesis of π-extended rubrenes 6 and 9, X-ray crystallographic analysis, computational detail, photophysical properties, fabrication and evaluation of OFETs, TG-DTA of rubrene 9, ^1H and ^{13}C NMR spectra (PDF)

Accession Codes

CCDC 2040996−2040999 contain the supplementary crystallographic data for this paper. These data can be obtained free of charge via www.ccdc.cam.ac.uk/data_request/cif, or by emailing data_request@ccdc.cam.ac.uk, or by contacting The Cambridge Crystallographic Data Centre, 12 Union Road, Cambridge CB2 1EZ, UK; fax: +44 1223 336033.

CCDC 2040996−2040999 contain the supplementary crystallographic data for this paper. These data can be obtained free of charge via www.ccdc.cam.ac.uk/data_request/cif.

https://doi.org/10.1021/jacs.2c11338
J. Am. Chem. Soc. 2023, 145, 658−666

AUTHOR INFORMATION

Corresponding Authors

Hideto Ito − *Department of Chemistry, Graduate School of Science, Nagoya University, Nagoya 464-8602, Japan*; Email: ito.hideto.p4@f.mail.nagoya-u.ac.jp

Kenichiro Itami − *Department of Chemistry, Graduate School of Science and Institute of Transformative Bio-Molecules (WPI-ITbM), Nagoya University, Nagoya 464-8602, Japan*; orcid.org/0000-0001-5227-7894; Email: itami@chem.nagoya-u.ac.jp

Authors

Wataru Matsuoka − *Department of Chemistry, Graduate School of Science, Nagoya University, Nagoya 464-8602, Japan*; Present Address: Department of Chemistry, Faculty of Science, Hokkaido University, Sapporo 060-0810, Japan; orcid.org/0000-0002-8342-249X

Kou P. Kawahara − *Department of Chemistry, Graduate School of Science, Nagoya University, Nagoya 464-8602, Japan*

David Sarlah − *Department of Chemistry, University of Illinois, Urbana, Illinois 61801, United States*; orcid.org/0000-0002-8736-8953

Complete contact information is available at: https://pubs.acs.org/10.1021/jacs.2c11338

Notes

The authors declare no competing financial interest.

ACKNOWLEDGMENTS

This work was supported by the ERATO program from JST (JPMJER1302 to K.I.), JST-CREST program (JPMJCR19R1 to H.I.), the JSPS KAKENHI (Grant No. JP21H01931), the Noguchi Research Foundation, and the Yazaki Memorial Foundation for Science and Technology, and the Foundation of public interest of Tatematsu (to H.I.). We thank Dr. Yasutomo Segawa for helping with the X-ray diffraction analysis. MS measurements were conducted using the resources of the Chemical Instrumentation Facility (CIF), Research Center for Materials Science (RCMS), Nagoya University. The computation was performed using Research Center for Computational Science, Okazaki, Japan (Project Nos.: 21-IMS-C070, 22-IMS-C069). ITbM is supported by the World Premier International Research Center Initiative (WPI), Japan. Fabrication of OFET devices and those evaluation were conducted using Custom Evaluation Service of OFET performance by Tokyo Chemical Industry, Co. Ltd. (TCI) in Japan.

REFERENCES

(1) For selected reviews, see: (a) Forrest, S. The path to ubiquitous and low-cost organic electronic appliances on plastic. *Nature* **2004**, *428*, 911−918. (b) Wang, C.; Dong, H.; Jiang, L.; Hu, W. Organic semiconductor crystals. *Chem. Soc. Rev.* **2018**, *47*, 422−500. (c) Klauk, H. Organic thin-film transistors. *Chem. Soc. Rev.* **2010**, *39*, 2643−2666.

(2) For selected reviews, see: (a) Someya, T.; Sekitani, T.; Iba, S.; Kato, Y.; Kawaguchi, H.; Sakurai, T. A large-area, flexible pressure sensor matrix with organic field-effect transistors for artificial skin applications. *Proc. Natl. Acad. Sci. U. S. A.* **2004**, *101*, 9966−9970. (b) Arias, A. C.; MacKenzie, J. D.; McCulloch, I.; Rivnay, J.; Salleo, A. Materials and applications for large area electronics: solution-based approaches. *Chem. Rev.* **2010**, *110*, 3−24. (c) Root, S. E.; Savagatrup, S.; Printz, A. D.; Rodriquez, D.; Lipomi, D. J. Mechanical properties of organic semiconductors for stretchable, highly flexible, and mechanically robust electronics. *Chem. Rev.* **2017**, *117*, 6467−6499.

(3) For selected reviews, see: (a) Wu, J.; Pisula, W.; Müllen, K. Graphenes as potential material for electronics. *Chem. Rev.* **2007**, *107*, 718−747. (b) Grzybowski, M.; Sadowski, B.; Butenschön, H.; Gryko, D. T. Synthetic applications of oxidative aromatic coupling—from biphenols to nanographenes. *Angew. Chem., Int. Ed.* **2020**, *59*, 2998−3027. (c) Sun, Z.; Ye, Q.; Chi, C.; Wu, J. Low band gap polycyclic hydrocarbons: from closed-shell near infrared dyes and semiconductors to open-shell radicals. *Chem. Soc. Rev.* **2012**, *41*, 7857−7889.

(4) For selected examples, see: (a) Podzorov, V.; Pudalov, V. M.; Gershenson, M. E. Field-effect transistors on rubrene single crystals with parylene gate insulator. *Appl. Phys. Lett.* **2003**, *82*, 1739−1741. (b) Sundar, V. C.; Zaumseil, J.; Podzorov, V.; Menard, E.; Willett, R. L.; Someya, T.; Gershenson, M. E.; Rogers, J. A. Elastomeric transistor stamps: Reversible probing of charge transport in organic crystals. *Science* **2004**, *303*, 1644−1646. (c) Podzorov, V.; Menard, E.; Borissov, A.; Kiryukhin, V.; Rogers, J. A.; Gershenson, M. E. Intrinsic charge transport on the surface of organic semiconductors. *Phys. Rev. Lett.* **2004**, *93*, No. 086602. (d) Takeya, J.; Yamagishi, M.; Tominari, Y.; Hirahara, R.; Nakazawa, Y.; Nishikawa, T.; Kawase, T.; Shimoda, T.; Ogawa, S. Very high-mobility organic single-crystal transistors with in-crystal conduction channels. *Appl. Phys. Lett.* **2007**, *90*, No. 102120.

(5) For selected examples, see: (a) Jurchescu, O. D.; Meetsma, A.; Palstra, T. T. M. Low-temperature structure of rubrene single crystals grown by vapor transport. *Acta Cryst. B* **2006**, *62*, 330−334. (b) Huang, L.; Liao, Q.; Shi, Q.; Fu, H.; Ma, J.; Yao, J. Rubrene micro-crystals from solution routes: their crystallography, morphology and optical properties. *J. Mater. Chem.* **2010**, *20*, 159−166. (c) Irkhin, P.; Biaggio, I. Direct imaging of anisotropic exciton diffusion and triplet diffusion length in rubrene single crystals. *Phys. Rev. Lett.* **2011**, *107*, No. 017402. (d) Najafov, H.; Lee, B.; Zhou, Q.; Feldman, L. C.; Podzorov, V. Observation of long-range exciton diffusion in highly ordered organic semiconductors. *Nat. Mater.* **2010**, *9*, 938−943. (e) Ma, L.; Zhang, K.; Kloc, C.; Sun, H.; Michel-Beyerle, M. E.; Gurzadyan, G. G. Singlet fission in rubrene single crystal: direct observation by femtosecond pump-probe spectroscopy. *Phys. Chem. Chem. Phys.* **2012**, *14*, 8307−8312. (f) Miyata, K.; Kurashige, Y.; Watanabe, K.; Sugimoto, T.; Takahashi, S.; Tanaka, S.; Takeya, J.; Yanai, T.; Matsumoto, Y. Coherent singlet fission activated by symmetry breaking. *Nat. Chem.* **2017**, *9*, 983−989. (g) Singh-Rachford, T. N.; Castellano, F. N. J. Pd(II) phthalocyanine-sensitized triplet−triplet annihilation from rubrene. *Phys. Chem. A* **2008**, *112*, 3550−3556. (h) Gray, V.; Dzebo, D.; Abrahamsson, M.; Albinsson, B.; Moth-Poulsen, K. Triplet−triplet annihilation photon-upconversion: towards solar energy applications. *Phys. Chem. Chem. Phys.* **2014**, *16*, 10345−10352. (i) Huang, Z.; Xu, Z.; Mahboub, M.; Liang, Z.; Jaimes, P.; Xia, P.; Graham, K. R.; Tang, M. L.; Lian, T. Enhanced near-infrared-to-visible upconversion by synthetic control of PbS nanocrystal triplet photosensitizers. *J. Am. Chem. Soc.* **2019**, *141*, 9769−9772. (j) Podzorov, V.; Menard, E.; Rogers, J. A.; Gershenson, M. E. Hall effect in the accumulation layers on the surface of organic semiconductors. *Phys. Rev. Lett.* **2005**, *95*, No. 226601. (k) Lee, B.; Chen, Y.; Fu, D.; Yi, H. T.; Czelen, K.; Najafov, H.; Podzorov, V. Trap healing and ultralow-noise Hall effect at the surface of organic semiconductors. *Nat. Mater.* **2013**, *12*, 1125−1129.

(6) For review, see: (a) Clapham, M. L.; Murphy, E. C.; Douglas, C. J. Synthesis and crystal engineering of rubrene and its derivatives. *Synthesis* **2021**, *53*, 461−474. For selected examples, see: (b) Braga, D.; Jaafari, A.; Miozzo, L.; Moret, M.; Rizzato, S.; Papagni, A.; Yassar, A. The rubrenic synthesis: the delicate equilibrium between tetracene and cyclobutene. *Eur. J. Org. Chem.* **2011**, *2011*, 4160−4169. (c) Uttiya, S.; Miozzo, L.; Fumagalli, E. M.; Bergantin, S.; Ruffo, R.; Parravicini, M.; Papagni, A.; Moret, M.; Sassella, A. Connecting molecule oxidation to single crystal structural and charge transport properties in rubrene derivatives. *J. Mater. Chem. C* **2014**, *2*, 4147−4155. (d) Dodge, J. A.; Bain, J. D.; Chamberlin, A. R. Regioselective

synthesis of substituted rubrenes. *J. Org. Chem.* **1990**, *55*, 4190−4198. (e) Allen, C. F. H.; Gilman, L. A synthesis of rubrene. *J. Am. Chem. Soc.* **1936**, *58*, 937−940. (f) Zhang, Z.; Ogden, W. A.; Young, V. G., Jr.; Douglas, C. J. Synthesis, electrochemical properties, and crystal packing of perfluororubrene. *Chem. Commun.* **2016**, *52*, 8127−8130. (g) McGarry, K. A.; Xie, W.; Sutton, C.; Risko, C.; Wu, Y.; Young, V. G., Jr.; Brédas, J.-L.; Frisbie, C. D.; Douglas, C. J. Rubrene-based single-crystal organic semiconductors: synthesis, electronic structure, and charge-transport properties. *Chem. Mater.* **2013**, *25*, 2254−2263. (h) Mamada, M.; Katagiri, H.; Sakanoue, T.; Tokito, S. Characterization of new rubrene analogues with heteroaryl substituents. *Cryst. Growth Des.* **2015**, *15*, 442−448. (i) Xie, G.; Hahn, S.; Rominger, F.; Freudenbergab, J.; Bunz, U. F. H. Synthesis and characterization of two different azarubrenes. *Chem. Commun.* **2018**, *54*, 7593−7596. Also see, ref 20

(7) For reported late-stage functionalizations of rubrene, see (a) Aubry, J. M.; Rigaudy, J.; Cuong, N. K. A water-soluble rubrene derivative: Synthesis, properties and trapping of $^1O_2$ in aqueous solution. *Photochem. Photobiol.* **1981**, *33*, 149−153. (b) Fagan, P. J.; Ward, M. D.; Caspar, J. V.; Calabrese, J. C.; Krusic, P. J. Synthesis and unusual properties of a helically twisted multiply metalated rubrene derivative. *J. Am. Chem. Soc.* **1988**, *110*, 2982−2983. (c) Freedman, D. A.; Matachek, J. R.; Mann, K. R. Ion pairing effects in the photochemistry of the cyclopentadienyl(η^6-benzene)osmium(II) cation. Synthesis and reactions of a synthetically useful intermediate: the cyclopentadienyltris(acetonitrile)osmium(II) cation. *Inorg. Chem.* **1993**, *32*, 1078−1080.

(8) (a) Ly, J.; Martin, K.; Thomas, S.; Yamashita, M.; Yu, B.; Pointer, C. A.; Yamada, H.; Carter, K. R.; Parkin, S.; Zhang, L.; Bredas, J.-L.; Young, E. R.; Briseno, A. L. Short excited-state lifetimes enable photo-oxidatively stable rubrene derivatives. *J. Phys. Chem. A* **2019**, *123*, 7558−7566. (b) Aubry, J.-M.; Pierlot, C.; Rigaudy, J.; Schmidt, R. Reversible binding of oxygen to aromatic compounds. *Acc. Chem. Res.* **2003**, *36*, 668−675.

(9) (a) Ito, H.; Ozaki, K.; Itami, K. Annulative π-extension (APEX): Rapid access to fused arenes, heteroarenes, and nanographenes. *Angew. Chem., Int. Ed.* **2017**, *56*, 11144−11164. (b) Ozaki, K.; Kawasumi, K.; Shibata, M.; Ito, H.; Itami, K. One-shot *K*-region-selective annulative π-extension for nanographene synthesis and functionalization. *Nat. Commum.* **2015**, *6*, 6251. (c) Matsuoka, W.; Ito, H.; Itami, K. Rapid access to nanographenes and fused heteroaromatics by palladium-catalyzed annulative π-extension reaction of unfunctionalized aromatics with diiodobiaryls. *Angew. Chem., Int. Ed.* **2017**, *56*, 12224−12228. (d) Kitano, H.; Matsuoka, W.; Ito, H.; Itami, K. Annulative π-extension of indoles and pyrroles with diiodobiaryls by Pd catalysis: Rapid synthesis of nitrogen-containing polycyclic aromatic compounds. *Chem. Sci.* **2018**, *9*, 7556.

(10) Matsuoka, W.; Ito, H.; Sarlah, D.; Itami, K. Diversity-oriented synthesis of nanographenes enabled by dearomative annulative π-extension. *Nat. Commun.* **2021**, *12*, 3940.

(11) (a) Jang, B.-B.; Lee, S. H.; Kafafi, Z. H. Asymmetric pentacene derivatives for organic light-emitting diodes. *Chem. Mater.* **2006**, *18*, 449−457. (b) Ebisawa, A.; Kitagawa, S.; Inoue, T. Compound for organic EL element and organic EL element. JP5101055B2, December 19, 2021.

(12) (a) Smyth, N.; Engen, D. V.; Pascal, R. A., Jr. Synthesis of longitudinally twisted polycyclic aromatic hydrocarbons via a highly substituted aryne. *J. Org. Chem.* **1990**, *55*, 1937−1940. (b) Rodríguez-Lojo, D.; Pérez, D.; Peña, D.; Guitián, E. One-pot synthesis of sterically congested large aromatic hydrocarbons via 1,4-diphenyl-2,3-triphenylyne. *Chem. Commun.* **2013**, *49*, 6274−6276. (c) Clevenger, R. G.; Kumar, B.; Menuey, E. M.; Lee, G.-H.; Patterson, D.; Kilway, K. V. A superior synthesis of longitudinally twisted acenes. *Chem. − Eur. J.* **2018**, *24*, 243−250. (d) Clevenger, R. G.; Kumar, B.; Menuey, E. M.; Kilway, K. V. Synthesis and structure of a longitudinally twisted hexacene. *Chem. − Eur. J.* **2018**, *24*, 3113−3116. (e) Xiao, Y.; Mague, J. T.; Schmehl, R. H.; Haque, F. M.; Pascal, R. A., Jr. Dodecaphenyltetracene. *Angew. Chem., Int. Ed.* **2019**, *58*, 2831−2833.

(13) (a) Qualizza, B. A.; Ciszek, J. W. Experimental survey of the kinetics of acene Diels−Alder reactions. *J. Phys. Org. Chem.* **2015**, *28*, 629−634. (b) Kjell, D. P.; Sheridan, R. S. Photochemical cycloaddition of *N*-methyltriazolinedione to naphthalene. *J. Am. Chem. Soc.* **1984**, *106*, 5368−5370. (c) Southgate, E. H.; Pospech, J.; Fu, J.; Holycoss, D. R.; Sarlah, D. Dearomative dihydroxylation with arenophiles. *Nat. Chem.* **2016**, *8*, 922−928. (d) Hernandez, L. W.; Klöckner, U.; Pospech, J.; Hauss, L.; Sarlah, D. Nickel-catalyzed dearomative trans-1,2-carboamination. *J. Am. Chem. Soc.* **2018**, *140*, 4503−4507. (e) Tang, C.; Okumura, M.; Zhu, Y.; Hooper, A. R.; Zhou, Y.; Lee, Y.-H.; Sarlah, D. Palladium-catalyzed dearomative syn-1,4-carboamination with Grignard reagents. *Angew. Chem., Int. Ed.* **2019**, *58*, 10245−10249. (f) Piacentini, P.; Bingham, T. W.; Sarlah, D. Dearomative ring expansion of polycyclic arenes. *Angew. Chem., Int. Ed.* **2022**, *61*, No. e202208014.

(14) (a) Ito, S.; Itoh, T.; Nakamura, M. Diastereoselective carbometalation of oxa- and azabicyclic alkenes under iron catalysis. *Angew. Chem., Int. Ed.* **2011**, *50*, 454−457. (b) Matsumoto, A.; Ilies, L.; Nakamura, E. Phenanthrene synthesis by iron-catalyzed [4+2] benzannulation between alkyne and biaryl or 2-alkenylphenyl Grignard reagent. *J. Am. Chem. Soc.* **2011**, *133*, 6557−6559.

(15) Mishima, D.; Nakanishi, H.; Tsuboi, Y.; Kishimoto, Y.; Yamanaka, Y.; Harada, A.; Togo, M.; Yamada, Y.; Muraoka, M.; Murata, M. Domino cross-Scholl reaction of tetracene with molecular benzene: Synthesis, structure, and mechanism. *Org. Lett.* **2021**, *23*, 7921−7926.

(16) For selected revies, see: (a) Watanabe, M.; Chen, K.-Y.; Chang, Y. J.; Chow, T. J. Acenes generated from precursors and their semiconducting properties. *Acc. Chem. Res.* **2013**, *46*, 1606−1615. (b) Dorel, R.; Echavarren, A. M. Strategies for the Synthesis of Higher Acenes. *Eur. J. Org. Chem.* **2017**, *2017*, 14−24. (c) Yamada, H.; Hayashi, H. Synthesis of oligoacenes using precursors for evaluation of their electronic structures. *Photochem. Photobiol. Sci.* **2022**, *21*, 1511−1532. (d) Yamada, H.; Kuzuhara, D.; Suzuki, M.; Hayashi, H.; Aratani, N. Synthesis and morphological control of organic semiconducting materials using the precursor approach. *Bull. Chem. Soc. Jpn.* **2020**, *93*, 1234−1267.

(17) Ma, L.; Galstyan, G.; Zhang, K.; Kloc, C.; Sun, H.; Soci, C.; Michel-Beyerle, M. E.; Gurzadyan, G. G. Two-photon-induced singlet fission in rubrene single crystal. *J. Chem. Phys.* **2013**, *138*, No. 184508.

(18) NCIPLOT: (a) Johnson, E. R.; Keinan, S.; Mori-Sánchez, P.; Contreras-García, J.; Cohen, A. J.; Yang, W. Revealing Noncovalent Interactions. *J. Am. Chem. Soc.* **2010**, *132*, 6498. (b) Contreras-García, J.; Johnson, E. R.; Keinan, S.; Chaudret, R.; Piquemal, J.-P.; Beratan, D. N.; Yang, W. NCIPLOT: A Program for Plotting Noncovalent Interaction Regions. *J. Chem. Theory Comput.* **2011**, *7*, 625. (c) Boto, R. A.; Peccati, F.; Laplaza, R.; Quan, C.; Carbone, A.; Piquemal, J.-P.; Maday, Y.; Contreras-García, J. NCIPLOT4: Fast, Robust, and Quantitative Analysis of Noncovalent Interactions. *J. Chem. Theory Comput.* **2020**, *16*, 4150.

(19) (a) Troisi, A. Ppreddiction of the absolute charge mobility of molecular semiconductors: The case of rubrene. *Adv. Mater.* **2007**, *19*, 2000−2004. (b) Nakayama, Y.; Uragami, Y.; Machida, S.; Koswattage, K. R.; Yoshimura, D.; Setoyama, H.; Okajima, T.; Mase, K.; Ishii, H. Full picture of valence band structure of rubrene single crystals probed by angle-resolved and excitation-energy-dependent photoelectron spectroscopy. *Appl. Phys. Express* **2012**, *5*, No. 111601.

(20) (a) Fratini, S.; Nikolka, M.; Salleo, A.; Schweicher, G.; Sirringhaus, H. Charge transport in high-mobility conjugated polymers and molecular semiconductors. *Nat. Mater.* **2020**, *19*, 491−502. (b) Dong, H.; Wang, C.; Hu, W. High performance organic semiconductors for field-effect transistors. *Chem. Commun.* **2010**, *46*, 5212−5222. (c) Wang, C.; Dong, H.; Hu, W.; Liu, Y.; Zhu, D. Semiconducting π-conjugated systems in field-effect transistors: A material odyssey of organic electronics. *Chem. Rev.* **2012**, *112*, 2208−2267. (d) Wang, C.; Dong, H.; Li, H.; Zhao, H.; Meng, Q.; Hu, W. Dibenzothiophene derivatives: From herringbone to lamellar packing motif. *Cryst. Growth Des.* **2010**, *10*, 4155−4160.

https://doi.org/10.1021/jacs.2c11338
J. Am. Chem. Soc. 2023, 145, 658−666

(21) (a) Ogden, W. A.; Ghosh, S.; Bruzek, M. J.; McGarry, K. A.; Balhorn, L.; Young, V.; Purvis, L. J.; Wegwerth, S. E.; Zhang, Z.; Serratore, N. A.; Cramer, C. J.; Gagliardi, L.; Douglas, C. J. Partial fluorination as a strategy for crystal engineering of rubrene derivatives. *Cryst. Growth Des.* **2017**, *17*, 643−658. (b) Sakamoto, Y.; Suzuki, T. Perfluorinated and half-fluorinated rubrenes: Synthesis and crystal packing arrangements. *J. Org. Chem.* **2017**, *82*, 8111−8116. (c) Li, J.; Ni, Z.; Zhang, X.; Li, R.; Dong, H.; Hu, W. Enhanced stability of a rubrene analogue with a brickwork packing motif. *J. Mater. Chem. C* **2017**, *5*, 8376−8379.

(22) (a) Anthony, J. E. Functionalized Acenes and Heteroacenes for Organic Electronics. *Chem. Rev.* **2006**, *106*, 5028−5048. (b) Anthony, J. E.; Eaton, D. L.; Parkin, S. R. A road map to stable, soluble, easily crystallized pentacene derivatives. *Org. Lett.* **2002**, *4*, 15−18. (c) Sheraw, C. D.; Jackson, T. N.; Eaton, D. L.; Anthony, J. E. Functionalized pentacene active layer organic thin-film transistors. *Adv. Mater.* **2003**, *15*, 2009−2011.

(23) (a) Li, L.; Tang, Q.; Li, H.; Yang, X.; Hu, W.; Song, Y.; Shuai, Z.; Xu, W.; Liu, Y.; Zhu, D. An ultra closely π-stacked organic semiconductor for high performance field-effect transistors. *Adv. Mater.* **2007**, *19*, 2613−2617. (b) Shukla, D.; Nelson, S. F.; Freeman, D. C.; Rajeswaran, M.; Ahearn, W. G.; Meyer, D. M.; Carey, J. T. Thin-film morphology control in naphthalene-diimide-based semiconductors: High mobility *n*-type semiconductor for organic thin-film transistors. *Chem. Mater.* **2008**, *20*, 7486−7491. (c) Ando, S.; Murakami, R.; Nishida, J.; Tada, H.; Inoue, Y.; Tokito, S.; Yamashita, Y. *n*-Type organic field-effect transistors with very high electron mobility based on thiazole oligomers with trifluoromethylphenyl groups. *J. Am. Chem. Soc.* **2005**, *127*, 14996−14997.

https://doi.org/10.1021/jacs.2c11338
J. Am. Chem. Soc. 2023, 145, 658−666